STEM CELLS TRANSLATIONAL MEDICINE®

TISSUE-SPECIFIC PROGENITOR AND STEM CELLS

Adult Lung Spheroid Cells Contain Progenitor Cells and Mediate Regeneration in Rodents With Bleomycin-Induced Pulmonary Fibrosis

ERIC HENRY,[a,b,*] JHON CORES,[a,b,*] M. TAYLOR HENSLEY,[a,*] SHIRENA ANTHONY,[c] ADAM VANDERGRIFF,[a,b] JAMES B.M. DE ANDRADE,[a] TYLER ALLEN,[a] THOMAS G. CARANASOS,[d] LEONARD J. LOBO,[e] KE CHENG[a,b]

Key Words. Adult lung stem cells • Mesenchymal stem cells • Pulmonary fibrosis • Spheroid cell culture

ABSTRACT

Lung diseases are devastating conditions and ranked as one of the top five causes of mortality worldwide according to the World Health Organization. Stem cell therapy is a promising strategy for lung regeneration. Previous animal and clinical studies have focused on the use of mesenchymal stem cells (from other parts of the body) for lung regenerative therapies. We report a rapid and robust method to generate therapeutic resident lung progenitors from adult lung tissues. Outgrowth cells from healthy lung tissue explants are self-aggregated into three-dimensional lung spheroids in a suspension culture. Without antigenic sorting, the lung spheroids recapitulate the stem cell niche and contain a natural mixture of lung stem cells and supporting cells. In vitro, lung spheroid cells can be expanded to a large quantity and can form alveoli-like structures and acquire mature lung epithelial phenotypes. In severe combined immunodeficiency mice with bleomycin-induced pulmonary fibrosis, intravenous injection of human lung spheroid cells inhibited apoptosis, fibrosis, and infiltration but promoted angiogenesis. In a syngeneic rat model of pulmonary fibrosis, lung spheroid cells outperformed adipose-derived mesenchymal stem cells in reducing fibrotic thickening and infiltration. Previously, lung spheroid cells (the spheroid model) had only been used to study lung cancer cells. Our data suggest that lung spheroids and lung spheroid cells from healthy lung tissues are excellent sources of regenerative lung cells for therapeutic lung regeneration. STEM CELLS TRANSLATIONAL MEDICINE *2015;4:1265–1274*

SIGNIFICANCE

The results from the present study will lead to future human clinical trials using lung stem cell therapies to treat various incurable lung diseases, including pulmonary fibrosis. The data presented here also provide fundamental knowledge regarding how injected stem cells mediate lung repair in pulmonary fibrosis.

INTRODUCTION

Lung diseases, such as chronic obstructive pulmonary disease (COPD) and idiopathic pulmonary fibrosis (IPF), are devastating conditions and, according to the World Health Organization, in the top five causes of mortality worldwide [1]. Stem cell therapy is a promising approach for lung regenerative medicine [2]. Pluripotent cells, such as embryonic stem cells or induced pluripotent stem cells, hold great differentiation and proliferation potential. However, clinical translation has been hampered by the potential teratogenic risk in human trials [3–5]. Current preclinical and clinical efforts are focusing on the infusions of adult stem cells isolated from human bone marrow, adipose tissue, placental tissue, or cord blood (referred to as mesenchymal stem cells or stromal cells) to treat patients with COPD, bronchopulmonary dysplasia, bronchiolitis obliterans, asthma, or acute lung injury [6–9]. However, a variety of resident lung stem cell types have been identified [10–15]. Compared with mesenchymal stem cells, the isolation and expansion of these resident lung stem cells for clinical usage remains a challenge. Antigenic sorting and purification are normally required. Furthermore, it is yet to be determined which surface marker or markers will identify the best cell sources for lung regenerative therapies.

We sought to develop a rapid, reproducible, and scalable method to generate clinically applicable amounts of resident lung progenitors. Multicellular spheroids represent a three-dimensional cell culture method frequently used in cancer biology [16, 17]. The spheroid method has also been used to generate neural stem cells [18] and cardiac stem cells [19]. It has also been reported that the spheroid microenvironment mimics the in vivo stem cell niche and is able to reprogram somatic cells into neural progenitor-like cells [20, 21]. We hypothesized that

[a]Department of Molecular Biomedical Sciences and Center for Comparative Medicine and Translational Research, College of Veterinary Medicine, and [c]Department of Biology, North Carolina State University, Raleigh, North Carolina, USA; [b]Joint Department of Biomedical Engineering, University of North Carolina at Chapel Hill, Chapel Hill, and North Carolina State University, Raleigh, North Carolina, USA; Divisions of [d]Cardiothoracic Surgery and [e]Pulmonary Diseases and Critical Care Medicine, University of North Carolina at Chapel Hill, Chapel Hill, North Carolina, USA

[*]Contributed equally.

Correspondence: Ke Cheng, Ph.D., Department of Molecular Biomedical Sciences and Center for Comparative Medicine and Translational Research, College of Veterinary Medicine, North Carolina State University, 1060 William Moore Drive, Raleigh, North Carolina 27607, USA. Telephone: 919-513-6157; E-Mail: ke_cheng@ncsu.edu or ke_cheng@unc.edu

Received March 27, 2015; accepted for publication July 29, 2015; published Online First on September 10, 2015.

1066-5099/2015/$20.00/0

http://dx.doi.org/10.5966/sctm.2015-0062

lung spheroids could be generated from healthy lung tissues and might contain lung progenitor cells suitable for therapeutic applications. In the present study, outgrowth cells from adult human lung tissues were self-aggregated into three-dimensional multicellular lung spheroids. When replated onto fibronectin-coated surfaces, the lung spheroids dissociated into single cells, which we termed "lung spheroid cells" (LSCs). Lung spheroids and LSCs represent natural mixtures of both lung progenitors and supporting stromal cells. Intravenous infusion of human LSCs ameliorated bleomycin-induced pulmonary fibrosis (PF) in immunodeficiency mice. In a rat model of pulmonary fibrosis, a head-to-head comparison revealed the therapeutic superiority of LSCs over adipose-derived mesenchymal stem cells with the same genetic background.

Materials and Methods

Generation of Lung Spheroids and Lung Spheroid Cells

Healthy human lung tissues were acquired from the Cystic Fibrosis and Pulmonary Diseases Research and Treatment Center at the University of North Carolina-Chapel Hill. Donor comorbidity is shown in supplemental online Table 1. An approximately 6 mm × 6 mm sample of distal lung tissue was separated and washed with phosphate-buffered saline (PBS) (Life Technologies, Carlsbad, CA, http://www.lifetechnologies.com). The tissue sample was then cut into smaller biopsy-size pieces and washed three times with PBS, followed by enzymatic digestion at 37°C in 5 mg/ml collagenase i.v. solution (Sigma-Aldrich, St. Louis, MO, http://www.sigmaaldrich.com) for 5 minutes. Iscove's modified Dulbecco's medium (IMDM; Life Technologies) containing 20% fetal bovine serum (FBS; Corning Life Sciences, Acton, MA, http://www.corning.com/lifesciences) was then added to the sample to inactivate the collagenase. Subsequently, the tissue samples were minced into smaller tissue explants (~0.5 × 0.5 mm) before plating. Approximately 50 pieces of tissue explants were then placed onto a fibronectin-coated plate with approximately 1.5 cm between each explant and covered with 2 ml of IMDM with 20% FBS overnight to aid their attachment onto the plate. The cultures were maintained in IMDM with 20% FBS, and a medium change was performed every other day. In approximately 1 week, cells started to outgrow from the tissue explants. Once these outgrowth cells were approximately 70%–80% confluent, they were harvested by 5–10 minutes of incubation with TryPLE Select (Life Technologies). The cells were then seeded into an ultra-low-attachment flask (Corning Life Sciences) at a density of 100,000 cells per cm^2 and cultured in IMDM with 10% FBS for spheroid formation. Phase-bright lung spheroids started to form in 3–7 days. Lung spheroids were then collected from the suspension culture and replated onto a fibronectin-coated surface to generate adherent LSCs. LSCs were cultured in IMDM containing 20% FBS, 50 μg/ml gentamicin, 2 mmol/l L-glutamine (Life Technologies), and 0.1 mmol/l 2-mercaptoethanol (Life Technologies). A cohort of LSCs were cultured in FBS-free medium containing 25 ng/ml epidermal growth factor (EGF; Shenandoah Biotechnology, Warwick, PA, http://www.shenandoah-bt.com) to test the effects of EGF on cell growth. The cells were passaged every 3–5 days. We used passage 2–3 LSCs for all in vitro and in vivo testing. Human pulmonary alveolar epithelial cells (HPAEpiC; ScienCell Research Laboratories, Carlsbad, CA, http://www.sciencellonline.com) and normal human dermal fibroblast cells (NHDFs; American Type Culture Collection, Manassas, VA, http://www.atcc.org) were cultured in the same medium as the control cells to human LSCs. Rat LSCs were generated from 6-week-old syngeneic Wistar-Kyoto rats using a similar protocol as for human LSCs. Rat adipose-derived mesenchymal stem cells (AD-MSCs) were derived from the same strain of rats as previously described [22]. Mouse PF-LSCs were generated from 6-week-old CD1 mice (Charles River Laboratories, Wilmington, MA, http://www.criver.com) 14 days after bleomycin instillation. Lung biopsy tissues from IPF patients were obtained from the IPF Clinic of University of North Carolina-Chapel Hill.

Flow Cytometry Analysis

To characterize the antigenic phenotypes of LSCs, flow cytometry was performed using a FACSCalibur or an LSR II flow cytometer (BD Biosciences, San Diego, CA, http://www.bdbiosciences.com) and analyzed using FlowJo software (TreeStar, Ashland, OR, http://www.flowjo.com). The cells were incubated with antibodies against CD31, CD34, CD45, CD90, CD105, Clara cell secretory protein (CCSP), pro-surfactant protein c (Pro-SPC), and aquaporin 5 for 60 minutes. Isotype-identical antibodies served as the negative control. Human bone marrow-derived mesenchymal stem cells (BM-MSCs) were obtained from Lonza (Walkersville, MD, http://www.lonza.com) as control cells for flow cytometry, and the BM-MSCs were cultured in the same LSC medium. To reveal the change in cell phenotype from spheroids to adherent cells, the lung spheroids were dissociated into single cells by 10–15 minutes of incubation with TryPEL Select (Life Technologies), and the dissociated cells were subjected to flow cytometry analysis.

Immunocytochemistry on Lung Spheroids and LSCs

LSCs were plated onto fibronectin-coated chamber slides (BD Biosciences) and subsequently fixed with 4% paraformaldehyde (PFA) before immunocytochemistry. Lung spheroids were mounted in Tissue-Tek O.C.T. compound (Sakura Finetek, Tokyo, Japan, http://www.sakura-finetek.com) and cryosectioned (5 μm). LSCs or lung spheroid sections were stained with the antibodies against CD31, CD34, CD45, CD90, CD105, CCSP, Pro-SPC, KRT5, p63, and aquaporin 5 and detected by fluorescein isothiocyanate (FITC)- or Texas Red-conjugated secondary antibodies (Abcam, Cambridge, MA, http://www.abcam.com/). Images were taken with an epifluorescent microscope (Olympus IX81; Olympus, Center Valley, PA, http://www.olympusamerica.com).

In Vitro Differentiation and Paracrine Assays

LSCs were transduced with viral particles of enhanced green fluorescent protein (EGFP; Vector Biolabs, Malvern, PA, http://www.vectorbiolabs.com). The cells were plated onto Matrigel (BD Biosciences) in serum-free media for observation of the formation of alveoli-like structures in vitro. Furthermore, LSCs on Matrigel were fixed with 4% PFA, followed by immunostaining on EGFP and aquaporin 5. Nuclei were counterstained with 4′,6-diamidino-2-phenylindole. To reveal the effects of LSC-secreted factors on lung epithelial cell survival, HPAEpiCs were cultured in control media (plain IMDM) or LSC-conditioned media. After 3 days, live and dead HPAEpiCs were stained with Calcein-AM and ethidium homodimer-1, respectively (Live/Dead Assay Kit; Life Technologies). The proangiogenic effects of LSC-conditioned media were studied by endothelial cell tube formation assay. Human umbilical vein endothelial cells (HUVECs; American Type Culture Collection) were seeded onto growth factor-reduced Matrigel in 96-well plates at a density of 2×10^4 cells per well. Next, 100 μl of plain

IMDM or conditioned media from human LSCs were added to the wells. After 4 hours, the wells were imaged with a Nikon TE-200 white light microscope (Nikon, Tokyo, Japan, http://www.nikon.com). The average tube length was then measured with NIH ImageJ software. To compare the secretion of human LSCs and NHDF cells, conditioned media from the two were collected and assayed with an antibody array (RayBiotech, Norcross, GA, http://www.raybiotech.com).

Animal Procedures

All animal work was compliant with the Institutional Animal Care and Use Committee at North Carolina State University. We randomized 6–8-week-old female severe combined immunodeficiency (SCID) mice (Charles River Laboratories) into the following three treatment groups (n = 6–7 mice for each group): (a) sham control: mice receiving 50 μl of PBS instilled intratracheally into the lungs; (b) Bleo + saline: mice receiving 0.7 U/kg body weight bleomycin in 50 μl of PBS (EMD Millipore, Bilerica, MA, http://www.emdmillipore.com/) instilled intratracheally into the lungs, followed by tail vein injection of 200 μl of PBS 24 hours later; and (c) Bleo + LSC: mice receiving 0.7 U/kg body weight bleomycin in 50 μl of PBS instilled intratracheally into the lungs, followed by tail vein injection of 1×10^6 human LSCs in 200 μl of PBS 24 hours later. A subset of animals in the Bleo + LSC group received LSCs labeled with green fluorescent cell tracker DiO (Life Technologies) or transduced with viral particles of EGFP (Vector Biolabs), facilitating histological detection of engrafted LSCs in the mouse lungs. At day 14, all mice were sacrificed, and their lungs were harvested for histological analysis, including hematoxylin and eosin (H&E) staining for alveolar thickening and infiltration, Masson's trichrome staining for fibrosis, terminal deoxynucleotidyl transferase dUTP nick-end labeling (TUNEL) assay (Sigma-Aldrich) for cell apoptosis, and immunohistochemistry staining on LSCs. To perform a head-to-head comparison of LSCs and another stem cell type in lung regeneration, 5×10^6 syngeneic rat LSCs or AD-MSCs were injected into 6-week-old female Wistar-Kyoto rats (Charles River Laboratories) with bleomycin-induced pulmonary fibrosis. The animals were euthanized 14 days later. The same H&E staining was performed to measure the degree of lung injury.

Histology

All the animals were sacrificed 14 days after treatment. The mouse lungs were harvested and frozen in Tissue-Tek O.C.T. compound (Sakura Finetek). Cryosections (5 μm thick) were prepared. For H&E staining, lung cryosections were stained for 2 minutes in hematoxylin and 30 seconds in eosin. Masson's trichrome staining was performed as per the manufacturer's instructions [HT15 Trichrome Staining (Masson) Kit; Sigma-Aldrich]. For immunofluorescence staining, lung cryosections were fixed with 4% PFA, blocked and permeabilized with Protein Block Solution (Dako, Carpinteria, CA, http://www.dako.com) containing 1% saponin (Sigma-Aldrich), and then stained with the following antibodies: rabbit anti-von Willebrand factor (Abcam), rabbit anti-Aquaporin 5 (Abcam), and chicken anti-GFP (Abcam). FITC or Texas-Red secondary antibodies were also obtained from Abcam. Images were taken using a Zeiss LSM 710 laser scanning confocal microscopy system (Carl Zeiss, Jena, Germany, http://www.zeiss.com). Apoptotic cells were detected by TUNEL assay using the In Situ Cell Death Detection Kit (Roche Diagnostics, Mannheim, Germany, http://www.roche-applied-science.com) according to the manufacturer's instructions.

Polymerase Chain Reaction Array

Using the RT^2 Profiler PCR Array System (Qiagen, Hilden, Germany, http://www.qiagen.com), we compared the expression of stem cell-related genes in human LSCs and HPAEpiCs. In brief, total RNA was extracted from explanted lungs and cDNA prepared from the total RNA mixture of three independent lungs using the RT^2 First Strand Kit (Qiagen). An experimental cocktail was prepared by adding cDNA to RT^2 qPCR Master Mix (Qiagen) within the 96-well polymerase chain reaction (PCR) array. Quantitative real-time PCR was performed with a Roche Light Cycler Real Time PCR System (Roche Diagnostics). A similar fibrosis-related gene PCR array was used to compare the expression of key genes involved in dysregulated tissue remodeling during the repair and fibrosis in the Bleo + saline and Bleo + LSC lungs.

Statistical Analysis

The results are presented as the mean $\pm$ SD, unless specified otherwise. Comparisons between any two groups were performed using 2-tailed unpaired Student's t tests. Comparisons among more than two groups were performed using one-way analysis of variance followed by post hoc Bonferroni correction. Differences were considered statistically significant at $p < .05$.

RESULTS

Generation of Lung Spheroids and LSCs

Using a three-dimensional suspension culture (Fig. 1A), we derived lung spheroids and LSCs from healthy adult human lung tissues. Both phase-bright and stromal-like cells started to outgrow from the lung tissue explants in 1 week after plating onto fibronectin-coated surfaces. Those outgrowth cells become confluent in ~2–3 weeks (Fig. 1B-I). When seeded onto an ultra-low-attachment surface (Corning Life Sciences) (to discourage cell attachment), the outgrowth cells spontaneously aggregated into three-dimensional lung spheroids (Fig. 1B-II). When replated onto a fibronectin-coated surface, the lung spheroids dissociated into single cells that we termed "lung spheroid cells" (Fig. 1B-III). One biopsy-size lung tissue sample can generate 10–20 million passage 0 LSCs. When maintained and passaged in IMDM with 20% FBS (Fig. 1B-IV), LSCs can further undergo 5–15 doublings within 15–50 days (Fig. 1C). Such cell yield and growth potential should suffice the requirement for clinical cell manufacturing.

Cell Phenotypes in Lung Spheroids and LSCs

Immunocytochemistry revealed an organized structure in the lung spheroids (Fig. 1D). Clusters of lung progenitor cells (e.g., Pro-SPC- and/or CCSP-positive cells, p63-positive cells, and KRT5-positive cells) reside in the spheroid core surrounded by CD105-positive and CD90-positive supporting (stromal-like) cells. These architectural features of lung spheroids resemble previously reported stem cell niches found in cardiac stem cell-formed spheroids [23]. Lung spheroids did not contain cells expressing hematopoietic markers such as CD45, CD31, and CD34 and had a low expression of the mature alveoli epithelial marker aquaporin 5. As the single-cell derivatives of lung spheroids, LSCs displayed a similar phenotypic profile. Flow cytometry analysis (Fig. 2A, 2C) revealed that LSCs were positive for CD105, CD90, Pro-SPC, and CCSP. Double staining confirmed that a subpopulation of LSCs was positive for both Pro-SPC and CCSP

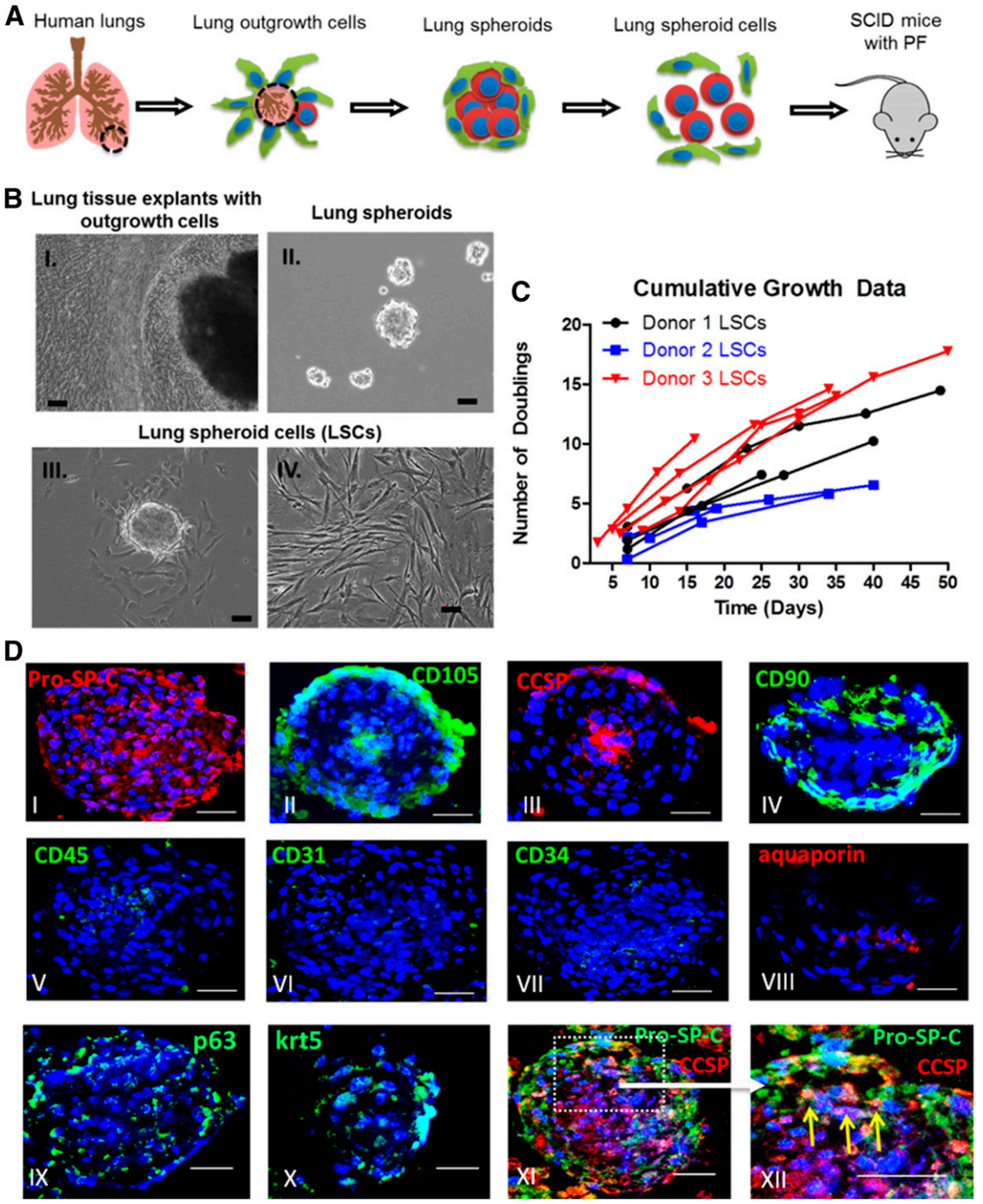

Figure 1. Generation of lung spheroids and lung spheroid cells. **(A):** Schematic showing the protocol to grow lung spheroids and lung spheroid cells. **(B-I):** Edge of lung tissue explants with outgrowth cells becoming confluent and ready to harvest. **(B-II):** Lung spheroids formed from outgrowth cells in suspension culture. **(B-III):** Plated lung spheroids onto fibronectin-coated surfaces to generate lung spheroid cells. **(B-IV):** Expansion of LSCs in suspension cultures. **(C):** Cumulative doubling for LSCs from three different donors. **(D):** Immunocytochemistry on lung spheroids. Scale bars = 50 μm. Abbreviations: LSCs, lung spheroid cells; PF, pulmonary fibrosis; SCID, severe combined immunodeficiency.

(Fig. 2D). LSCs are negative for hematopoietic cell markers CD45, CD31, CD34, and express a negligible percentage of the mature lung epithelial marker aquaporin 5. These compound data suggest that LSCs represent a selective mixture of lung progenitor cells and supporting cells. The phenotype of LSCs was distinct from that of BM-MSCs, because the latter did not express Pro-SPC or CCSP (supplemental online Fig. 1). To reveal the changes of cell phenotype from spheroids to adherent cells, we dissociated lung spheroids into single cells and then performed flow cytometry analysis. The results indicated a similar phenotype, except for slightly higher Pro-SPC expression at the spheroid stage (supplemental online Fig. 2). Immunocytochemistry on LSCs confirmed the flow cytometry results (Fig. 2B). To enable histological detection, a cohort of LSCs were transduced with EGFP viral particles. We confirmed that EGFP transduction did not affect the phenotype of LSCs (supplemental online Fig. 3).

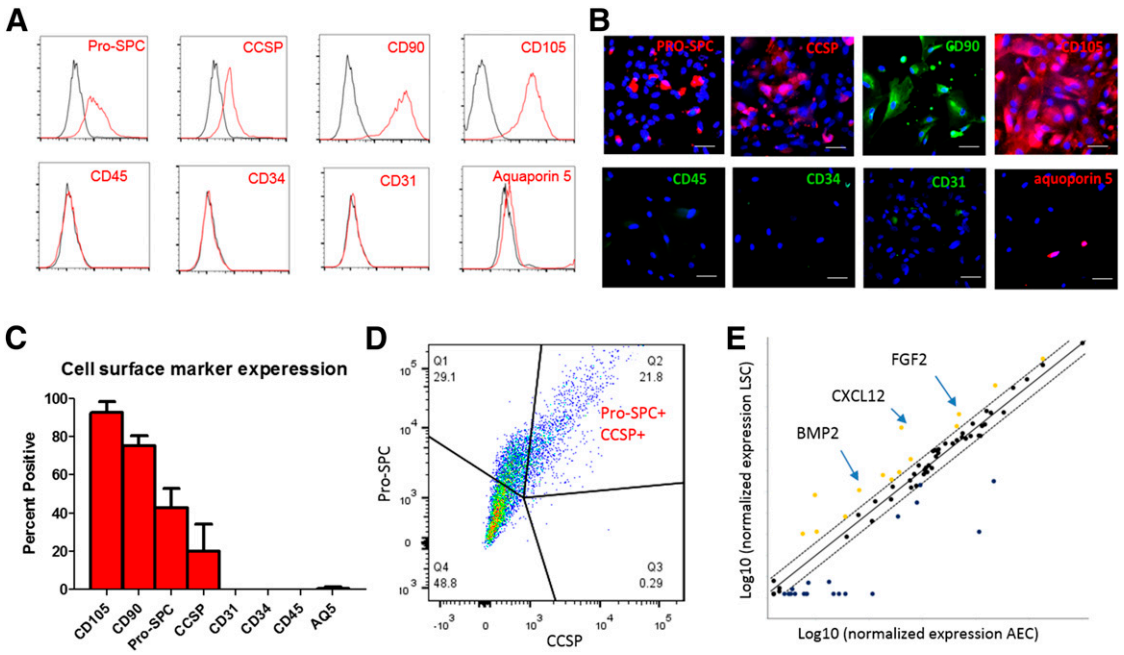

Figure 2. Lung spheroid cells contain lung progenitor cells. **(A):** Representative flow cytometry plots of LSCs for expression of CD31, CD34, CD45, CD90, CD105, CCSP, Pro-SPC, and aquaporin 5. Black lines indicate isotype controls; red lines, antibodies. **(B):** Immunocytochemistry staining of LSCs for the same markers. **(C):** Pooled data for the expression of the same markers (n = 3 lung donors). **(D):** Double staining of Pro-SPC and CSSP in LSCs. **(E):** Polymerase chain reaction array showing relative expression of stem cell genes in human LSCs and alveolar epithelial cells. Scale bars = 10 μm. Abbreviations: AEC, alveolar epithelial cell; AQ5, aquaporin 5; *BMP2*, bone morphogenetic protein 2; *CXCL12*, C-X-C motif chemokine 12; *FGF2*, fibroblast growth factor 2; Q, quartile.

Using a stemness-related gene PCR array, we compared the gene expression of human LSCs and HPAEpiCs (Fig. 2E). Multiple genes were upregulated in LSCs compared with HPAEpiCs, such as bone morphogenetic protein 2, stromal cell-derived factor 1 (also known as C-X-C motif chemokine 12), and fibroblast growth factor 2.

In Vitro Differentiation and Paracrine Assays

When cultured on Matrigel (BD Biosciences), LSCs self-assembled into alveoli-like structures (Fig. 3A). Immunostaining revealed that LSCs expressed aquaporin 5 (Fig. 3B, overlay of red/green with open arrowheads,) and acquired mature lung epithelial cell morphology. Nondifferentiated LSCs (Fig. 3B, green with solid arrowheads) remained positive for Pro-SPC (supplemental online Fig. 4, white arrow). Conditioned media from LSCs promoted survival or proliferation of human lung epithelial cells (Fig. 3C) and tube formation of human endothelial cells on Matrigel (LSC-conditioned media vs. control media, 237.8 $\pm$ 32.7 μm vs. 108.7 $\pm$ 81.1 μm; $p < .05$; Fig. 3D), suggesting a prosurvival and proangiogenic role of LSC-secreted factors. A cytokine array (Fig. 3E) revealed that compared with control cells (NHDFs), human LSCs secreted higher concentrations of proangiogenic factors such as insulin-like growth factor binding protein 2, hepatocyte growth factor, and brain-derived neurotrophic factor.

Regenerative Potential of LSCs in Mice With Pulmonary Fibrosis

The animal study design is outlined in Figure 4A. Pulmonary fibrosis was induced in SCID mice by intratracheal instillation of bleomycin; 24 hours later, the animals received an intravenous infusion of 1×10^6 human LSCs or saline control. The animals were followed up for another 14 days and then sacrificed for endpoint analysis. The macroscopic view of the explanted lungs revealed significant tissue damage (dense dark spots) in the Bleo + saline lungs (Fig. 4B). In contrast, the LSC-treated lungs (Bleo + LSC group) were similar to the lungs in the sham group. H&E staining (Fig. 4C) revealed that LSC treatment significantly reduced fibrous thickening (by Ashcroft score; Bleo + saline vs. Bleo + LSC, 5.7 $\pm$ 1.0 vs. 4.3 $\pm$ 0.7; Fig. 4E) and tissue infiltration (Bleo + saline vs. Bleo + LSC, 11.6 $\pm$ 5.7 vs. 4.3 $\pm$ 4.8; Fig. 4F). Masson's trichrome staining confirmed the reduction of fibrosis with LSC treatment (Fig. 4D, blue).

Mechanisms of LSC-Mediated Lung Protection and Regeneration

LSC engraftment reduced tissue apoptosis in the bleomycin-treated lungs. LSC engraftment (DiO-labeled; Fig. 5A, green) decreased the numbers of TUNEL-positive apoptotic cells (Fig. 5A, red nuclei) in the bleomycin-treated lungs (area without LSC vs. area with LSC, 1.9% $\pm$ 0.5% vs. 0.7% $\pm$ 0.2% of total nuclei). Such protection was seen in epithelial, stromal, and endothelial cell types in the lungs (supplemental online Fig. 5). In contrast, LSC treatment increased angiogenesis in the bleomycin-treated lungs: more von Willebrand factor-positive vasculatures were detected in the LSC-treated lungs (Bleo + saline vs. Bleo + LSC, 6.0 $\pm$ 2.3 vs. 11.8 $\pm$ 3.3 per high power field; Fig. 5B). Moreover, a greater number of blood vessels were formed around LSCs than in other areas without the presence of LSCs (supplemental online Fig. 6). These results were consistent with the prosurvival and proangiogenic effects of LSCs observed in vitro (Fig. 3). Although some injected human LSCs acquired mature lung epithelial cell phenotypes (e.g., EGFP-positive LSCs coexpressed differentiation of the lung epithelial cell marker aquaporin 5 [Fig. 5C, white arrows; supplemental online Fig. 7, inset b]), some LSCs remained positive for Pro-SPC (supplemental online Fig. 7, inset b). To reveal

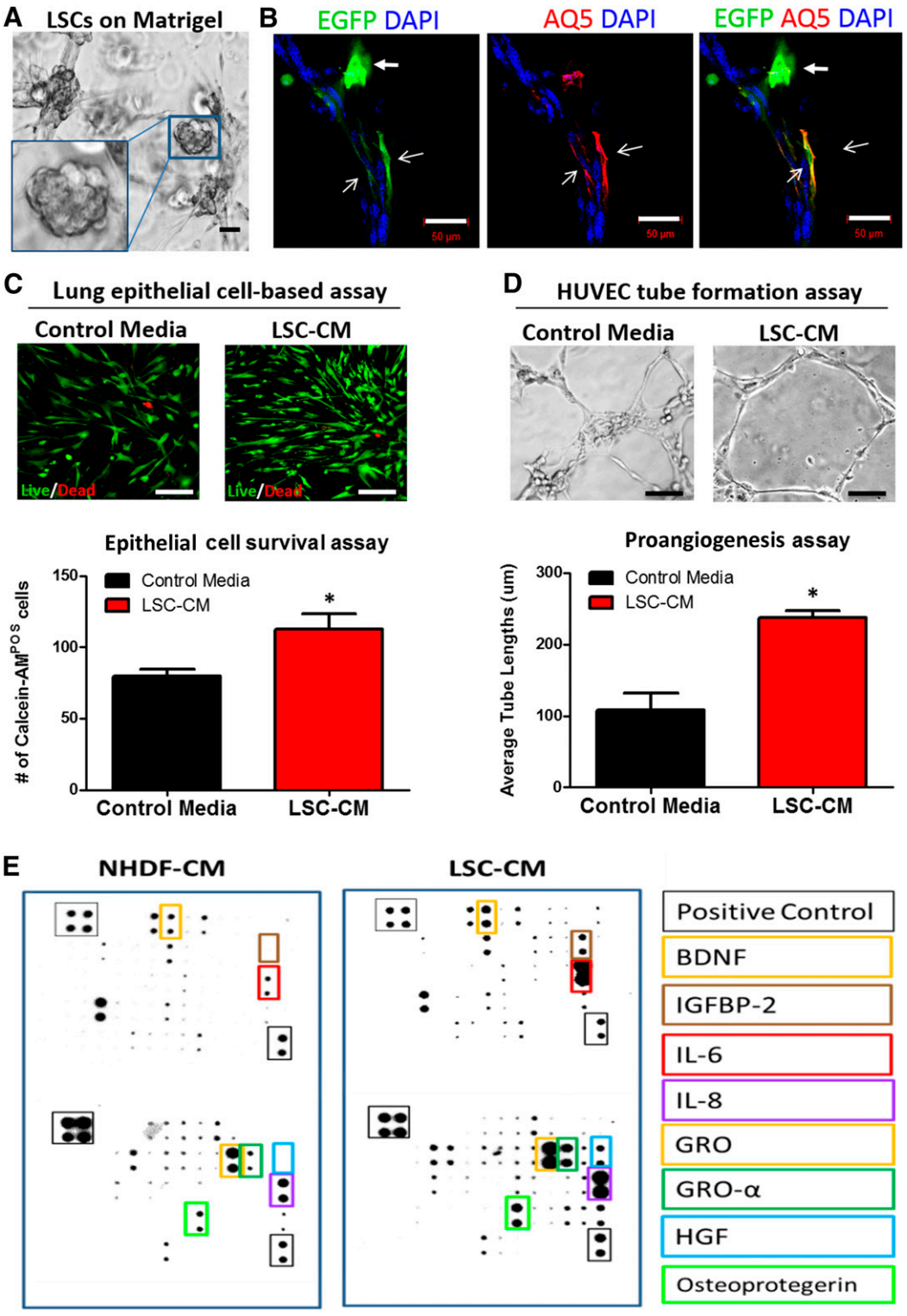

Figure 3. In vitro differentiation and paracrine assays of lung spheroid cells. **(A):** LSCs grown on Matrigel and displaying alveoli-like structures (inset). **(B):** LSCs grown on Matrigel expressed aquaporin 5 (red). **(C):** Human lung epithelial cells cultured in control media and LSC-CM and stained for live (green)/dead (red) assay. **(D):** HUVEC tube formation assay on Matrigel surface in control or conditioned media from LSCs. Data are presented as mean ± SD. All experiments were run in triplicate, unless noted otherwise. Scale bars = 50 μm. *, $p < .05$ compared with the control media group. **(E):** Representative antibody array images showing the proteins presenting in the CM from LSCs and NHDF cells. Abbreviations: AQ5, aquaporin 5; BDNF, brain-derived neurotrophic factor; CM, conditioned media; DAPI, 4′,6-diamidino-2-phenylindole; EGFP, enhanced green fluorescent protein; GRO, growth-regulated protein; HGF, hepatocyte growth factor; HUVEC, human umbilical vein endothelial cell; IGFBP2, insulin-like growth factor binding protein 2; IL, interleukin; LSCs, lung spheroid cells; POS, positive; NHDF, normal human dermal fibroblast cell.

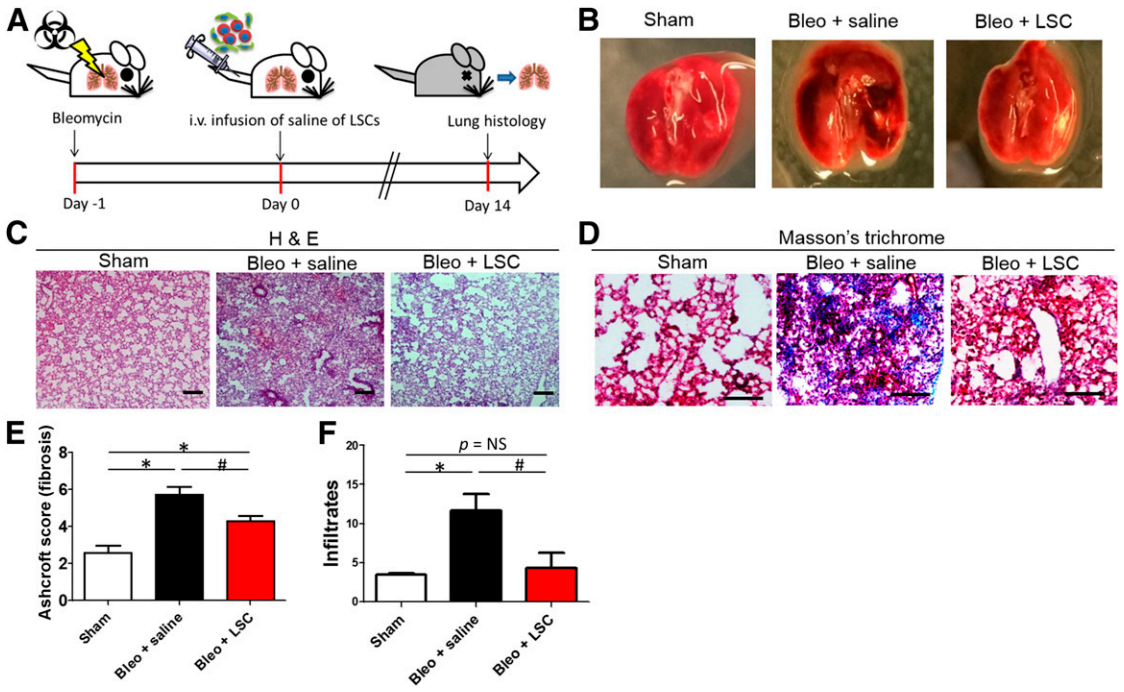

Figure 4. Therapeutic benefits of human LSCs in mice with bleomycin-induced pulmonary fibrosis. **(A):** Schematic showing the design of the mouse studies. **(B):** Macroscopic views of explanted lungs 14 days after LSC or saline treatment. H&E staining **(C)** and Masson's trichrome staining (D) were performed on the lungs. **(E):** Quantitation of fibrous thickening by Ashcroft score from the H&E staining images (n = 6–7 animals per group). **(F):** Quantitation of tissue infiltrates from the H&E staining images (n = 6–7 animals per group). Data are presented as mean ± SD. Scale bars = 100 μm. *, $p < .05$ compared with the sham group; #, $p < .05$ compared with the Bleo + saline group. Abbreviations: Bleo, bleomycin; H&E, hematoxylin and eosin; LSCs, lung spheroid cells.

the overall impact of LSC treatment on pulmonary fibrosis, we extracted RNA from the lungs from the Bleo + LSC and Bleo + saline groups. Quantitative PCR array revealed that LSC treatment attenuated the expression of fibrotic genes in the bleomycin-treated lungs (Fig. 5D; supplemental online Table 2).

Therapeutic Superiority of LSCs Over AD-MSCs

Because most current clinical trials are using MSCs to treat IPF and COPD, we sought to compare the therapeutic potencies of LSCs and AD-MSCs. To rule out donor variability, we derived rat LSCs and AD-MSCs from the syngeneic Wistar-Kyoto (WKY) rat strains, because these rats share the same genetic background. Rat LSCs share a similar antigenic phenotype with their human counterparts, with consistent expression of CD105, CD90, Pro-SPC, and CCSP (supplemental online Fig. 8). At 24 hours after bleomycin instillation, WKY rats were randomized to receive saline, rat LSCs, or rat AD-MSCs (Fig. 6A). Consistent with previous reports, H&E staining indicated that AD-MSC therapy reduced infiltrates by 14 days after cell therapy (Fig. 6B–6D, black bars) compared with the saline control (Fig. 6B–6D, white bars). A trend was also seen toward the reduction of fibrotic thickening (by Ashcroft score). However, the highest therapeutic effects were observed in the rats that received LSCs; they expressed the smallest degree of fibrotic thickening and tissue infiltration (Fig. 6B–6D, red bars). These data suggest that LSCs are superior to AD-MSCs in treating rats with PF.

Discussion

The past decade witnessed a burst of studies on identifying endogenous lung stem cells [24]. Many cell types in the lung, including basal cells, club cells, and alveolar type II cells, have been proposed as lung stem/progenitor cells. However, mesenchymal cells (from bone marrow, adipose tissues, umbilical cord) are still the major players in on-going cell-based clinical trials for treating lung diseases, due, at least in part, to the ease of isolating and propagating these cells.

Multicellular spheroids have been used as a method to generate neural and cardiac stem cells. A recent report indicated infusion of cardiosphere-derived cells in patients with a mild-to-moderate heart attack reduced scar and increased viable tissue [25]. To date, lung spheroids have only been recognized as a method to grow lung cancer cells [26]. In the present study, we have shown that lung spheroids from healthy lungs represent a robust method to generate therapeutic lung progenitor cells. The cell yield and growth potential of LSCs are suitable for both autologous and allogeneic applications (Fig. 1). No antigenic sorting is required. LSCs represent a natural mixture of both lung progenitor cells and supporting cells (Fig. 2). The origin of LSCs is yet to be determined. The expression of CD105, CD90, Pro-SPC, and CCSP identified human LSCs, suggesting that they might contain lung mesenchymal stem/stromal cells (CD105+/CD90+), alveolar progenitor cells (Pro-SPC+), and airway progenitor cells (CSSP+). LSCs are distinct from MSCs: human MSCs express CD105 and CD90 but not Pro-SPC or CCSP (supplemental online Fig. 1). A subfraction of LSCs was dual positive for Pro-SPC and CSSP, suggesting they might represent a population of bronchioalveolar stem cells. This natural mixture of lung progenitor cells could be a result of the ex vivo cell culture process. The three-dimensional spheroid culture might enrich the stem cell populations. Alternatively, mature lung epithelial cells can revert into progenitor cells, a process resembling the dedifferentiation of lung cells into stem cells in vivo

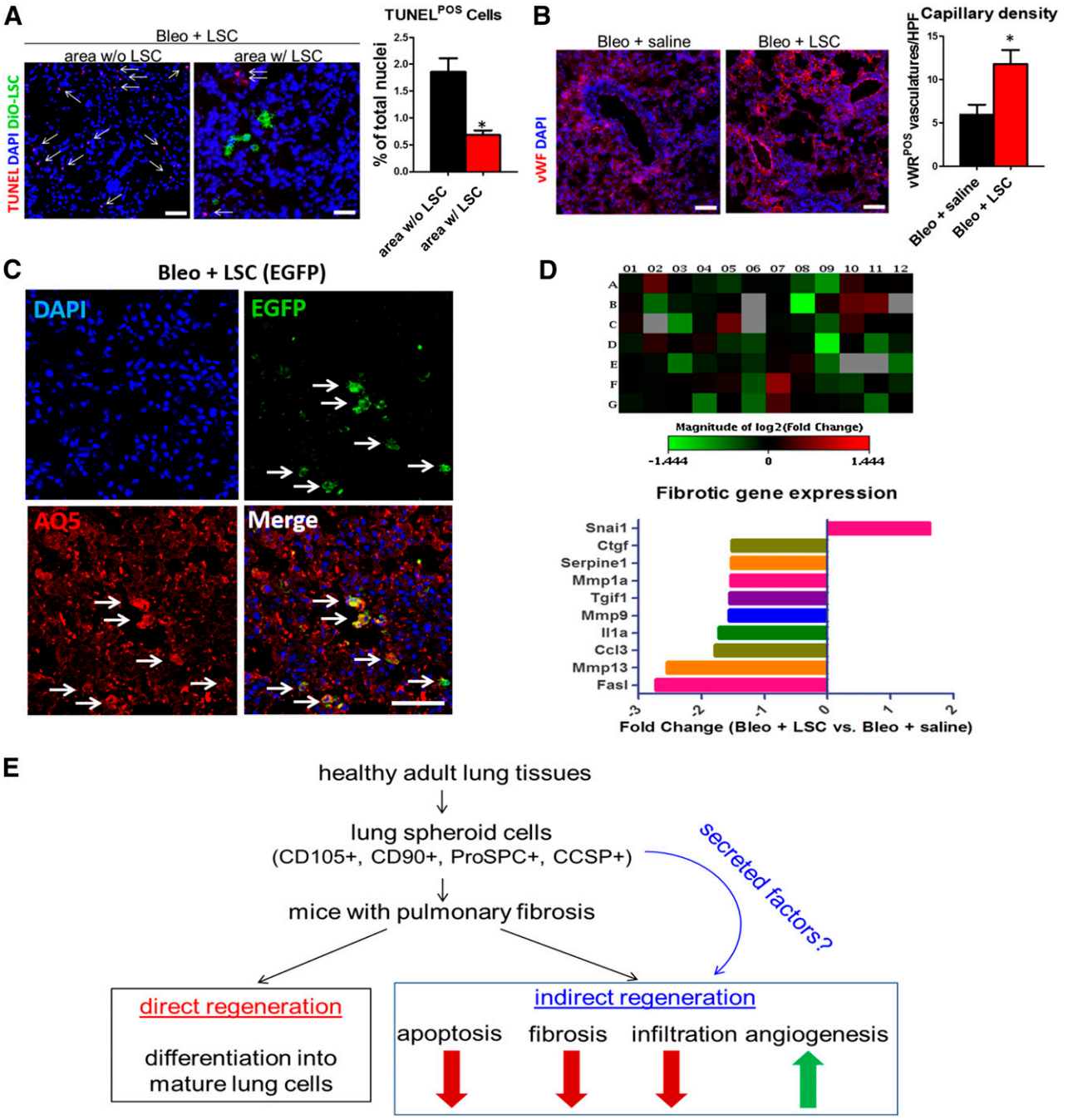

Figure 5. Mechanisms underlying the therapeutic effects of LSCs in pulmonary fibrosis. **(A):** Representative confocal images showing the numbers of apoptotic cells (red nuclei) in area with and without LSC engraftment (green) (n = 4 animals per group). **(B):** Representative confocal images showing vWF-positive vasculature (red) in the lungs treated with saline or LSCs (n = 4 animals per group). **(C):** Representative confocal images showing engrafted EGFP-positive LSCs coexpress mature lung epithelial cell marker aquaporin 5. **(D):** Quantitative polymerase chain reaction array showing the expression of fibrosis-related genes in lungs treated with saline or LSCs (using a cutoff criterion of a fold change >1.5). **(E):** Proposed mechanisms for LSC-mediated lung repair in pulmonary fibrosis. Data are presented as mean ± SD. Scale bars = 20 μm. *, $p < .05$ using unpaired Student's t tests. Abbreviations: AQ5, aquaporin 5; Bleo, bleomycin; DAPI, 4′,6-diamidino-2-phenylindole; EGFP, enhanced green fluorescent protein; HPF, high power field; LSCs, lung spheroid cells; POS, positive; TUNEL, terminal deoxynucleotidyl transferase dUTP nick-end labeling; vWF, von Willebrand factor; w/, with; w/o, without.

[27]. LSCs were able to form alveoli-like structures and acquired mature lung epithelial phenotypes/morphologies in vitro, suggesting their differentiation potential (Fig. 3A, 3B). The conditioned media from LSCs promoted lung epithelial cell survival (Fig. 3C) and endothelial cell tube formation (Fig. 3D). Cytokine array data suggested that LSCs might promote lung regeneration through the secretion of antiapoptotic and proangiogenic factors and cytokines (Fig. 3E).

To test the regenerative potential of LSCs in vivo, we created a pulmonary fibrosis model in mice via intratracheal instillation of bleomycin. The use of immunodeficiency (SCID) mice makes it possible to test human LSCs without fear of rejection. No complications

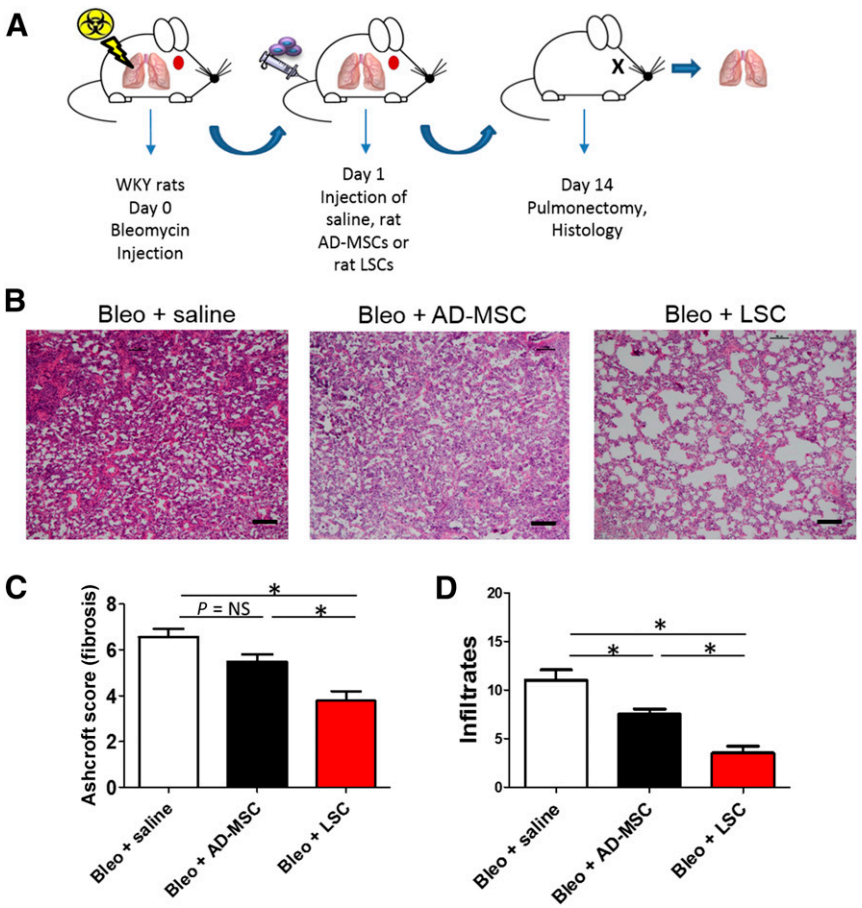

Figure 6. Therapeutic superiority of LSCs over AD-MSCs. **(A):** Schematic showing the design of the rat studies. **(B):** Hematoxylin and eosin staining of rat lung sections 14 days after treatment with saline, AD-MSCs, or LSCs. **(C):** Quantitation of fibrous thickening by Ashcroft score from H&E staining images (n = 5 animals per group). **(D):** Quantitation of tissue infiltrates from H&E staining images (n = 5 animals per group). Data are presented as mean ± SD. Scale bars = 100 μm. *, $p < .05$. Abbreviations: AD-MSCs, adipose-derived mesenchymal stem cells; Bleo, bleomycin; LSCs, lung spheroid cells; WKY, Wistar-Kyoto.

were observed in the mice that received the LSC infusion. No tumors or ectopic tissues were observed in any of the animals treated with LSCs. Treatment with LSCs inhibited fibrosis (Fig. 4E), infiltration (Fig. 4F), and cell apoptosis (Fig. 5A) but promoted angiogenesis (Fig. 5B). LSCs engrafted and acquired mature lung phenotypes in the recipient lungs (Fig. 5C), although such small engraftment and differentiation incidents seem insufficient to explain the overall benefits. Mounting lines of evidence suggest that injected stem cells regenerate damaged tissues through indirect paracrine mechanisms [28]. We speculate LSCs secrete beneficial factors that modulate the environment and recruit endogenous repair mechanisms (Fig. 5E).

Because MSCs are the most popular cells in clinical trials for lung diseases, we performed a head-to-head comparison of rat LSCs and AD-MSCs in the same rat model of PF (Fig. 6). LSCs outperformed AD-MSCs in reducing fibrotic thickening and tissue infiltration in PF lungs. The underlying mechanisms need to be further elucidated. Because these were derived from adult lungs instead of adipose tissue, we speculate that LSCs are predesignated to differentiate into lung cells and promote endogenous lung regeneration.

Our study also had several limitations. First, we did not isolate the MSC population from the LSC mixture and then perform a head-to-head comparison of the two in vitro and in vivo. Second, the injection of stem cells at 24 hours after bleomycin injection might not be clinically relevant, because IPF is considered a chronic disease. Third, the optimal media for culturing LSCs warrants further investigation. Normally FBS-free media containing EGF is used for lung epithelial stem cell culture. We compared LSCs cultured in two conditions: (a) 25 ng/ml EGF and no FBS; and (b) 20% FBS and no EGF. The morphologies of LSCs were similar in those two conditions, albeit the cells cultured in 20% FBS media grew faster (supplemental online Fig. 9). These yet-to-be elucidated questions will be the effort of our future directions in this line of research. As an autologous product, we anticipate an IPF patient will come to the clinic, and a lung biopsy will be performed to generate the tissues required for LSC culture. These autologous cells will then be reintroduced into the same patient by intravenous injection. To this end, we have confirmed that LSCs can be derived from mouse (supplemental online Fig. 10) and human (supplemental online Fig. 11) lungs with PF. Future studies are also warranted to elucidate the regenerative potential of PF lung-derived LSCs, the origin of LSCs, and the mechanisms underlying their therapeutic benefits and to translate these findings into a clinically relevant large animal model of lung disease.

Conclusion

We identified lung spheroids from healthy human lungs as a great source of lung progenitor cells that can be used for therapeutic

lung regeneration. Lung spheroids represent a simple and highly reproducible method to generate therapeutic lung cells without antigenic sorting.

Acknowledgments

We thank S. Randell, L. Fulcher, and E. Powell at University of North Carolina at Chapel Hill for assistance in obtaining human lung samples. This work was supported by funding from the National Institutes of Health, American Heart Association, North Carolina State University (NC State) Chancellor's Faculty Excellence Program, NC State Center for Comparative Medicine and Translational Researches, and NC State Kenan Foundation Regenerative Medicine Grant.

Author Contributions

E.H.: conception/design, collection and/or assembly of data, data analysis and interpretation, manuscript writing; J.C. and M.T.H.: conception/design, collection and/or assembly of data, data analysis and interpretation; S.A., A.V., J.B.M.d.A., and T.A.: collection and/or assembly of data; T.G.C. and L.J.L.: provision of study material or patients; K.C.: conception/design, financial support, data analysis and interpretation, manuscript writing, final approval of manuscript.

Disclosure of Potential Conflicts of Interest

K.C. has had a provisional patent filed. The other authors indicated no potential conflicts of interest.

References

1 Cottin V. Interstitial lung disease. Eur Respir Rev 2013;22:26–32.

2 Yang J, Jia Z. Cell-based therapy in lung regenerative medicine. Regen Med Res 2014;2:7.

3 Takahashi K, Tanabe K, Ohnuki M et al. Induction of pluripotent stem cells from adult human fibroblasts by defined factors. Cell 2007; 131:861–872.

4 Takahashi K, Yamanaka S. Induction of pluripotent stem cells from mouse embryonic and adult fibroblast cultures by defined factors. Cell 2006;126:663–676.

5 Thomson JA, Itskovitz-Eldor J, Shapiro SS et al. Embryonic stem cell lines derived from human blastocysts. Science 1998;282:1145–1147.

6 Moodley Y, Atienza D, Manuelpillai U et al. Human umbilical cord mesenchymal stem cells reduce fibrosis of bleomycin-induced lung injury. Am J Pathol 2009;175:303–313.

7 Ortiz LA, Dutreil M, Fattman C et al. Interleukin 1 receptor antagonist mediates the antiinflammatory and antifibrotic effect of mesenchymal stem cells during lung injury. Proc Natl Acad Sci USA 2007;104:11002–11007.

8 Ortiz LA, Gambelli F, McBride C et al. Mesenchymal stem cell engraftment in lung is enhanced in response to bleomycin exposure and ameliorates its fibrotic effects. Proc Natl Acad Sci USA 2003;100:8407–8411.

9 Tzouvelekis A, Paspaliaris V, Koliakos G et al. A prospective, non-randomized, no placebo-controlled, phase Ib clinical trial to study the safety of the adipose derived stromal cells-stromal vascular fraction in idiopathic pulmonary fibrosis. J Transl Med 2013;11:171.

10 Desai TJ, Brownfield DG, Krasnow MA. Alveolar progenitor and stem cells in lung development, renewal and cancer. Nature 2014;507:190–194.

11 Kajstura J, Rota M, Hall SR et al. Evidence for human lung stem cells. N Engl J Med 2011; 364:1795–1806.

12 Kim CF, Jackson EL, Woolfenden AE et al. Identification of bronchioalveolar stem cells in normal lung and lung cancer. Cell 2005;121:823–835.

13 Wansleeben C, Barkauskas CE, Rock JR et al. Stem cells of the adult lung: Their development and role in homeostasis, regeneration, and disease. Wiley Interdiscip Rev Dev Biol 2013;2:131–148.

14 Barkauskas CE, Cronce MJ, Rackley CR et al. Type 2 alveolar cells are stem cells in adult lung. J Clin Invest 2013;123:3025–3036.

15 Hogan BL, Barkauskas CE, Chapman HA et al. Repair and regeneration of the respiratory system: Complexity, plasticity, and mechanisms of lung stem cell function. Cell Stem Cell 2014; 15:123–138.

16 Fennema E, Rivron N, Rouwkema J et al. Spheroid culture as a tool for creating 3D complex tissues. Trends Biotechnol 2013;31:108–115.

17 LaBarbera DV, Reid BG, Yoo BH. The multicellular tumor spheroid model for high-throughput cancer drug discovery. Expert Opin Drug Discov 2012;7:819–830.

18 Deleyrolle L, Reynolds B. Isolation, expansion, and differentiation of adult mammalian neural stem and progenitor cells using the neurosphere assay. In: Gordon D, Scolding NJ, eds. Neural Cell Transplantation. New York, NY: Humana Press, 2009:91–101.

19 Marbán E. Breakthroughs in cell therapy for heart disease: Focus on cardiosphere-derived cells. Mayo Clin Proc 2014;89:850–858.

20 Su G, Zhao Y, Wei J et al. The effect of forced growth of cells into 3D spheres using low attachment surfaces on the acquisition of stemness properties. Biomaterials 2013;34:3215–3222.

21 Su G, Zhao Y, Wei J et al. Direct conversion of fibroblasts into neural progenitor-like cells by forced growth into 3D spheres on low attachment surfaces. Biomaterials 2013;34:5897–5906.

22 Li TS, Cheng K, Malliaras K et al. Direct comparison of different stem cell types and subpopulations reveals superior paracrine potency and myocardial repair efficacy with cardiosphere-derived cells. J Am Coll Cardiol 2012;59:942–953.

23 Li T-S, Cheng K, Lee S-T et al. Cardiospheres recapitulate a niche-like microenvironment rich in stemness and cell-matrix interactions, rationalizing their enhanced functional potency for myocardial repair. Stem Cells 2010;28:2088–2098.

24 Kotton DN, Morrisey EE. Lung regeneration: Mechanisms, applications and emerging stem cell populations. Nat Med 2014;20:822–832.

25 Makkar RR, Smith RR, Cheng K et al. Intracoronary cardiosphere-derived cells for heart regeneration after myocardial infarction (CADUCEUS): A prospective, randomised phase 1 trial. Lancet 2012;379:895–904.

26 Amann A, Zwierzina M, Gamerith G et al. Development of an innovative 3D cell culture system to study tumour–stroma interactions in non-small cell lung cancer cells. PLoS One 2014;9:e92511.

27 Tata PR, Mou H, Pardo-Saganta A et al. Dedifferentiation of committed epithelial cells into stem cells in vivo. Nature 2013;503:218–223.

28 Chimenti I, Smith RR, Li T-S et al. Relative roles of direct regeneration versus paracrine effects of human cardiosphere-derived cells transplanted into infarcted mice. Circ Res 2010;106:971–980.

See www.StemCellsTM.com for supporting information available online.